

Production and Observation of the Dissipative Trapped-Ion Instability

J. Slough, G. A. Navratil, and A. K. Sen

Plasma Physics Laboratory, Columbia University, New York, New York 10027

(Received 13 July 1981)

A new, steady-state linear mirror machine has been constructed which produces a low-density, low-temperature hydrogen plasma in the collisionality regime of the dissipative trapped-ion instability. This instability was seen and identified through the observed dependence of wave amplitude on trapped fraction, axial and radial position, and collisionality and through the scaling of real frequency with trapped fraction.

PACS numbers: 52.35.Py, 52.25.Gj, 52.35.Kt

Since the prediction of an instability due to the presence of trapped particles in toroidal systems was made by Kadomtsev and Pogutse,¹ there has been concern that these instabilities (particularly the dissipative trapped-ion instability²) would limit the particle and energy containment time of tokamak fusion reactions. Although recent results from the neutral-beam-heated Princeton Large Torus³ tokamak have indicated operation in the parameter regime where the trapped-ion instability would be expected to occur, there has been no positive identification of this instability. The experimental observation of this or any other instability in tokamaks is made difficult, if not impossible, as a result of the inherent complexity of the magnetic geometry and the resulting complex mode structure,⁴ the appearance of turbulence, and the lack of good local diagnostics in such hot plasmas.

With the above limitations in mind, we have simulated the required reactorlike conditions of low collisionality in a new low-temperature (10 eV) and low-density (10^9 cm^{-3}) linear device which allowed us to produce the dissipative trapped-ion instability and study it with local Langmuir probe diagnostics. This new linear machine⁵ represents an extension of the parameter-space regime accessible to linear devices. Previous devices both here at Columbia University^{6,7} and elsewhere^{8,9} have operated in the more collisional regime of the trapped-electron instability.

As will be shown, the trapped-ion instability, like the trapped-electron instability,^{6,7} does not depend fundamentally on the particular complex geometry of toroidal devices. The only essential conditions required are that ions and electrons be trapped and have the proper collisionality and bounce frequency. The Columbia University linear machine⁵ was designed to meet these requirements. Other parameters which can contribute to the instability are electron and ion temperature gradients and particularly grad- B drifts.

The criteria that the device must meet for excitation of the trapped-ion instability can be stated simply as follows. The first condition is that

$$\omega_r \ll \omega_{bi}, \quad (1)$$

where ω_r is the real frequency and approximately equal to $\frac{1}{2} \delta \omega_e^*$ (Ref. 2), with δ the fraction of trapped particles and ω_e^* the electron diamagnetic drift frequency, and ω_{bi} is the trapped-ion bounce frequency. In these experiments, we found that ω_r was approximately $0.1\omega_{bi}$ which is satisfactory. The second condition is that

$$\nu_i/\epsilon \ll \omega_{bi}; \quad \epsilon = 1 - R^{-1}. \quad (2)$$

Here ν_i/ϵ is the ion detrapping collision frequency and R is the mirror ratio. For typical operating conditions in our experiment of $T_i = 5 \text{ eV}$, $R = 2.5$, $L = 50 \text{ cm}$, and $n_i = 10^9 \text{ cm}^{-3}$ we obtain ν_i/ϵ approximately equal to $10^{-3}\omega_{bi}$. The third condition

$$\nu_e/\epsilon \ll \omega_{be} \quad (3)$$

is for trapped electrons and was easily met in our device with ν_e/ϵ approximately equal to $10^{-3}\omega_{be}$.

If the above conditions are satisfied, one can derive the following dispersion relation applicable to a one-dimensional, infinite plasma with a density and electron temperature gradient²:

$$1 - \frac{\delta}{1+\tau} \left\langle \frac{\omega - \omega_e^* [1 + \eta_e (x^2 - 3/2)]}{\omega + i\nu_e/\epsilon x^3 + i\nu_{en}} \right\rangle - \frac{\delta\tau}{1+\tau} \frac{\omega + \omega_e^*/\tau}{\omega + i\nu_i/\epsilon + i\nu_{in}} = 0, \quad (4)$$

where $\tau = T_e/T_i$, $x = v/v_{th}$, and the above average is over a Maxwellian distribution. Included in the dispersion relation is a correction for detrapping collisions with neutral particles. Solutions of the above dispersion relation relevant to our experimental parameters are shown in Fig. 1. One can easily see the strong role of neutral collisions as the instability is damped for $\nu_{en} > 5 \times 10^4 \text{ sec}^{-1}$.

The Columbia University linear machine pro-

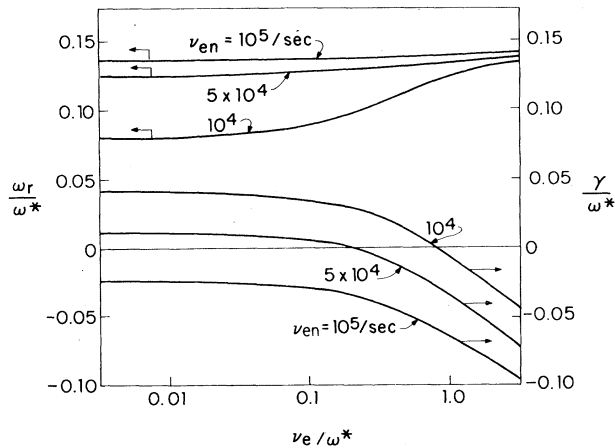


FIG. 1. Growth rate γ and real frequency ω_r as a function of collisionality. Curves are for various values of electron-neutral collision frequency ν_{en} . Here $\omega_e^* = 1.2 \times 10^5/\text{sec}$, $\delta = 0.25$, $\epsilon = \frac{1}{2}$, $\eta_e = 1$, and $T_e = T_i$.

duces a quiescent, low-neutral-density hydrogen plasma and is shown schematically in Fig. 2 along with a plot of the magnetic field on axis. A continuous hydrogen plasma was produced in a uniform 3.3 kG magnetic field by an $\vec{E} \parallel \vec{B}$ discharge source. The plasma was guided through two differential pumping stages into the mirror cell region where the neutral hydrogen background was 2×10^{-6} Torr. This pressure was sufficiently low to reduce $\nu_{in} \lesssim \nu_{ie}$ at the 10^9 cm^{-3} densities used in the experiment. The ions also acquired a Maxwellian 5 eV temperature as they fell down the potential gradient which existed between the source and cell with elastic neutral collisions between the first and second differential pumping

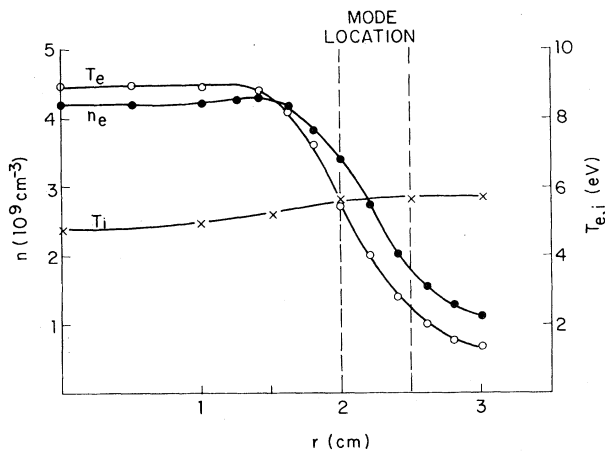


FIG. 3. Typical density (closed circles), electron temperature (open circles), and ion temperature (crosses) profiles as a function of radius.

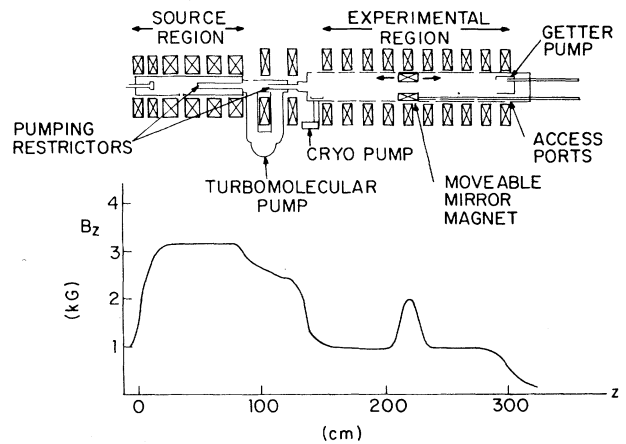


FIG. 2. Schematic diagram of the linear device and a plot of the axial magnetic field with the movable mirror magnet on.

stages providing the necessary scattering. In the mirror cell we then studied a quiescent hydrogen plasma, with radial profiles of T_i , T_e , and n_e given in Fig. 3. Plasma density can be varied from 5×10^8 to 10^{10} cm^{-3} by changing the discharge current in the source with no appreciable change in the electron and ion temperature profiles. At the 1 kG field used in all of these experiments the electron diamagnetic drift frequency for $m = 1$ modes in the center of the density gradient was roughly constant at $f_e^* \approx 50 \text{ kHz}$. Effects of the

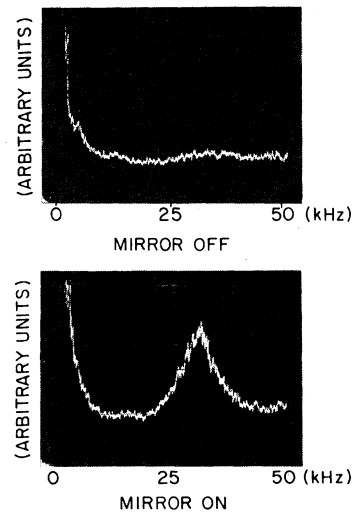


FIG. 4. Frequency spectra of density fluctuations on the plasma edge with no trapped particles and roughly 25% trapped particles. The $m = 1$ mode is clearly observed.

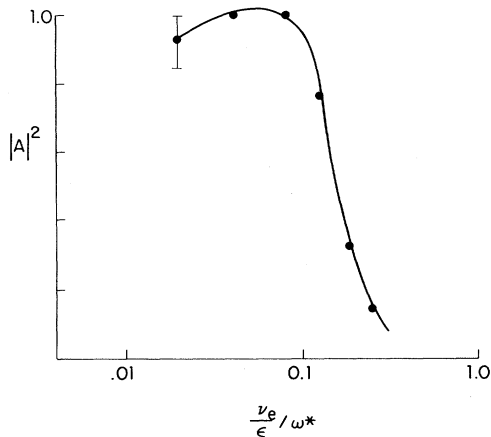


FIG. 5. Relative mode amplitude squared as a function of the effective detrapping collision frequency ν_e/ϵ where $\delta = 0.20$.

magnetic curvature in the mirror regions have been neglected because calculations indicate that the ratio $\langle\omega_D\rangle/\omega_{e^*} \lesssim 0.005$, where $\langle\omega_D\rangle$ is the bounce-averaged curvature drift frequency. The plasma potential and resulting radial electric field were measured with Langmuir probes. From this one finds an $\vec{E} \times \vec{B}$ plasma rotation frequency, f_E , of approximately 25 kHz for the edge of the plasma.

With the second mirror turned on, the trapped-ion instability was clearly present as shown in Fig. 4. The instability was located radially on the edge of the plasma as shown in Fig. 3; its maximum coincided with the point of largest density gradient where the local value of the trapped fraction was approximately 20%. The instability was seen only marginally outside of the mirror cell where there were no trapped particles.

The trapped-ion instability should be damped by an increase in collisionality whether from neutral or Coulomb collisions. The latter dependence was observed by changing the plasma density and the results are shown in Fig. 5. The former dependence was observed by bleeding neutral H_2 into the mirror cell. The damping of the instability as the neutral collisionality was increased is shown in Fig. 6.

It was possible by changing the density to change the trapped fraction while keeping the magnetic geometry, temperature, and all other plasma parameters, except collisionality, the same. Since the real frequency of the trapped-ion instability is proportional to the trapped fraction and only weakly dependent on the collisionality, one

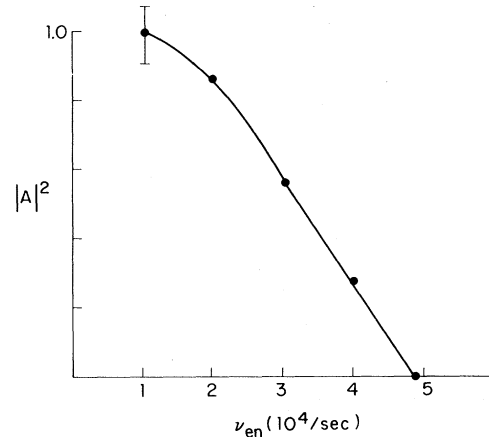


FIG. 6. Relative mode amplitude squared as a function of electron-neutral collisionality, ν_{en} , where $\tilde{n}/n(\text{max}) \approx 25\%$, $f_r = 10$ kHz, $\delta = 0.25$, and $n_e = 2 \times 10^9 \text{ cm}^{-3}$.

should observe a shift in frequency with a change in trapped fraction. This shift was observed and is shown in Fig. 7.

The azimuthal mode number, m , was found to be equal to 1. Also, the parallel wavelength λ_{\parallel} was estimated from the standing wave axial structure of the mode. For a mirror cell length of $L = 80$ cm, we found λ_{\parallel} to be approximately 160 cm which is consistent with $\lambda_{\parallel} \sim 2L$. The corresponding parallel phase velocity was approximately 1×10^6 cm/sec which was less than the average transition speed of approximately 5×10^6 cm/sec, thereby avoiding ion Landau damping.

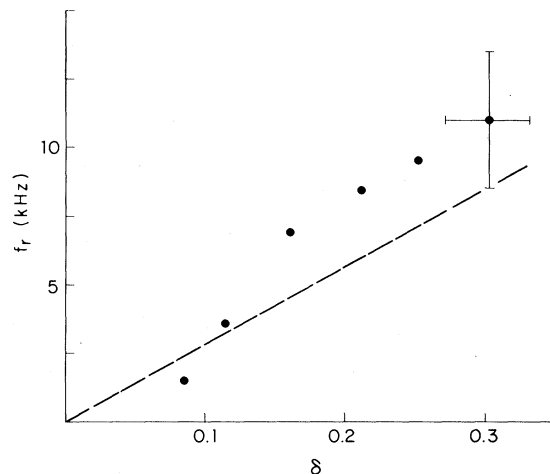


FIG. 7. Observed trapped-ion mode frequency f_r , corrected for Doppler shifts as a function of trapped fraction, δ . Dashed line is $f_r = \delta f_e^*/2$.

Thus, the observation and identification of the trapped-ion instability has been seen in many ways. These are as follows: the dependence of the wave amplitude on collisionality was in the range and in the manner predicted for the trapped-ion instability; the instability existed only on the density gradient and it existed only when and where there were trapped particles; and the observed frequency of the trapped-ion instability was at the predicted frequency ($\frac{1}{2}\delta\omega_e^*$) and showed the proper dependence on trapped fraction. Although other experiments have operated in the proper collisionality range for the trapped-ion instability^{10,11} they were unable to satisfy requirement (1), $\omega_r \ll \omega_{bi}$. This experiment satisfied all of the requirements and provides the first positive identification of the dissipative trapped-ion instability.

This research was supported by the National Science Foundation under Grant No. ECS79-17033 and by the Research Corporation.

¹B. B. Kadomtsev and O. P. Pogutse, *Zh. Eksp. Teor. Fiz.* **51**, 1734 (1966) [*Sov. Phys. JETP* **24**, 1172 (1967)].

²M. N. Rosenbluth, D. W. Ross, and D. P. Kostomarov, *Nucl. Fusion* **12**, 3 (1972).

³H. Eubank *et al.*, in *Proceedings of the Seventh International Conference on Plasma Physics and Controlled Nuclear Fusion Research, Innsbruck, Austria, 1978* (International Atomic Energy Agency, Vienna, Austria, 1979), p. 167.

⁴R. Marchand, W. M. Tang, and G. Rewoldt, *Phys. Fluids* **23**, 1164 (1980).

⁵G. A. Navratil, J. Slough, and A. K. Sen, to be published.

⁶S. C. Prager, T. C. Marshall, and A. K. Sen, *Plasma Phys.* **17**, 785 (1975).

⁷D. P. Dixon, A. K. Sen, and T. C. Marshall, *Plasma Phys.* **20**, 225 (1977).

⁸D. Brossier, P. Deschamps, and C. Renard, *Phys. Rev. Lett.* **26**, 124 (1971).

⁹D. P. Grubb and G. A. Emmert, *Phys. Fluids* **22**, 770 (1979).

¹⁰M. Okabayashi and R. Freeman, *Phys. Fluids* **15**, 359 (1972).

¹¹J. R. Drake, *Phys. Fluids* **20**, 1013 (1977).

Helical and Nonhelical Turbulent Dynamos

M. Meneguzzi

Centre National de la Recherche Scientifique and Section d'Astrophysique, Division de la Physique, Centre d'Etudes Nucléaires de Saclay, F-91191 Gif-Sur-Yvette, France

and

U. Frisch

Centre National de la Recherche Scientifique, Observatoire de Nice, F-06007 Nice, France

and

A. Pouquet^(a)

Centre National de la Recherche Scientifique, Observatoire de Meudon, F-92190 Meudon, France

(Received 13 April 1981)

Direct numerical simulations of three-dimensional magnetohydrodynamic turbulence with kinetic and magnetic Reynolds numbers up to 100 are presented. Spatially intermittent magnetic fields are observed in a flow with nonhelical driving. Small-scale helical driving produces strong large-scale nearly force-free magnetic fields.

PACS numbers: 51.60.+a, 47.65.+a, 52.30.+r

The stretching of magnetic field lines by turbulent motions in a conducting fluid is one of the most frequently invoked mechanisms for the generation of the magnetic fields of the earth, the sun, stars, and galaxies.¹ It may also lead to undesirable magnetic fields in the liquid sodium cooling system of large breeder reactors.^{2,3} When the magnetic Reynolds number R^M exceeds a critical value R_c^M , the stretching is sufficiently

strong to overcome the diffusive effect of Joule dissipation, thereby leading to dynamo action. Specifically, consider a statistically stationary turbulent flow with no magnetic field. Let a weak seed magnetic field be introduced. For $R^M < R_c^M$, the same stationary state is recovered asymptotically in time. For $R^M > R_c^M$, the flow bifurcates to a new statistically stationary state. In this nonlinear dynamo regime, the Lorentz force, by

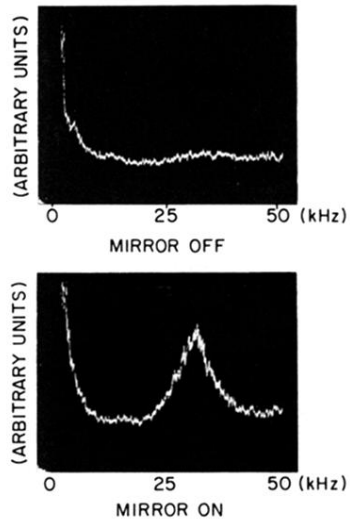


FIG. 4. Frequency spectra of density fluctuations on the plasma edge with no trapped particles and roughly 25% trapped particles. The $m = 1$ mode is clearly observed.